J. Fluid Mech. (1991), *vol.* 223, *pp.* 135–163
Printed in Great Britain

Two-layer hydraulics: a functional approach

By STUART B. DALZIEL
Department of Applied Mathematics and Theoretical Physics, University of Cambridge, Silver Street, Cambridge CB3 9EW, UK

(Received 15 June 1989 and in revised form 4 June 1990)

A new approach for investigating two-layer hydraulic exchange flows in channels is introduced. The approach is based on the functional formalism of Gill (1977) and applied to the flow through a contraction in width and to flow over a simple sill. The sill geometry is an extension of that looked at by earlier workers, in particular Farmer & Armi (1986) who used a Froude-number-plane approach. In the present paper a simple relationship between the composite Froude number and the *hydraulic functional* is derived, though the functional approach may also be applied to channels where a Froude number is not readily defined. The ability to trace roots of this functional from one reservoir to the other is a prerequisite for the flow to be realizable. Two *hydraulic transitions* are required for the flow to be fully controlled and the exchange flow rate to be *maximal*. If only one hydraulic transition is present, the flow is governed by the conditions in one of the reservoirs and the exchange flow rate is found to be *submaximal*. The flow along a channel is found to be very sensitive to small departures from symmetry about a horizontal plane. The response of the interface to the introduction of a net (barotropic) flow is found to be a discontinuous function of the strength of the forcing for some range of sill heights.

1. Introduction

The study of two-layer hydraulics is important in a whole range of fluid flows, from thermally driven exchange flows through doorways to oceanic currents such as the flow through the Strait of Gibraltar (the density difference is provided by a difference in salinity between the Mediterranean Sea and the Atlantic Ocean). Despite the obvious need to understand these flows, in particular when the flow is *hydraulically controlled* (the exchange flow is then *maximal*), there have been comparatively few investigations of this steady, nonlinear phenomenon. In contrast the related single-layer flow has a large established body of literature describing and analysing all the different aspects of the flow.

The work of Stommel & Farmer (1953) on overmixing and the exchange of salinity between an estuary and the open ocean prompted much of the more recent work in this area. Wood (1968, 1970) introduced a number of key ideas, the most notable being that two distinct (separate) hydraulic transitions may occur when there are two flowing layers. The most compete works to date are those by Armi and Farmer (Armi 1986; Armi & Farmer 1986; Farmer & Armi 1986). A thorough review of earlier attempts to analyse two-layer flows is given in Armi (1986).

Utilizing a quasi-linear approach, Armi (1986) showed the relevance of the composite Froude number to such flows. Solutions for channels of rectangular cross-section and simple along-channel geometry were obtained using a formulation in the layer Froude-number plane. These results demonstrated a fundamental difference

between flow through a contraction and that over a sill; earlier workers had viewed these two situations as equivalent (e.g. Mehrotra 1973).

Armi & Farmer (1986) and Farmer & Armi (1986) expanded on the work of Armi (1986) to investigate a broader range of along-channel geometries. This work has been applied to the flow through the Strait of Gibraltar (Farmer & Armi 1986; Armi & Farmer 1987, 1988) as an explanation of the observed internal flow features.

The approach of Armi & Farmer is difficult to apply to channels with complex along-channel geometries and is not appropriate for channels in which the layer and composite Froude numbers vary across the width (e.g. rotating channels, Dalziel 1990). In addition to being less general, the Froude-number-space formulation obscures the physical reasons why some flows may not be realized.

This paper offers an alternative formulation of the two-layer hydraulic problem to illuminate more clearly the fundamental features of such flows. The new formulation is readily applicable to channels of non-rectangular cross-section (Dalziel 1988) and channels in rotating systems (Dalziel 1988, 1990). The formulation in this paper is based on the functional formalism expounded by Gill (1977) for *hydraulic-type* problems in his investigation of the effects of rotation on single-layer flows. This formalism has been shown to be equivalent to the quasi-linear approach for non-dissipative single-layer flows by Pratt & Armi (1987).

In §§2 and 3 we summarize the essential features of two-layer hydraulics, introducing the necessary equations and discussing how disturbances are communicated along channels. In §4 we derive the two-layer hydraulic functional, giving details of its structure, the relationship with the Froude number, and how the functional may be used to solve two-layer exchange flows. The results of Armi (1986), Armi & Farmer (1986) and Farmer & Armi (1986) are confirmed in §§5 and 6 (respectively), using the functional approach, before being extended in §6 to a broader range of along-channel geometries. This extension is essential to understand when the limits analysed by Farmer & Armi may be applied. The energetics of two-layer sill flow is also discussed, showing that such flows are necessarily dissipative. Finally, in §7, the conditions giving rise to maximal and submaximal exchange flows are detailed.

2. Model geometry and equations

Consider two large reservoirs connected by a channel of varying width and depth. One reservoir contains fluid of density ρ_1 and the other of a lower density ρ_2. The fluids are Boussinesq ($0 < \rho_1 - \rho_2 \ll \frac{1}{2}(\rho_1 + \rho_2)$), the density difference driving an exchange flow along the channel. Following normal hydraulic practice, we shall assume that the flow is irrotational (except for thin vortex sheets at the interface; the analysis for flows with vertical vorticity is similar, but beyond the scope of this paper) and incompressible. Viscous effects are assumed negligible, except for energy dissipation within internal hydraulic jumps and bores. Further, variations in the height of the interface between the two layers and variations in the channel geometry occur over lengthscales large compared with the depth of the channel. These assumptions enable us to apply the shallow-water approximation under which the pressure is hydrostatic within each layer.

For later convenience we non-dimensionalize the equations with respect to the channel geometry at the shallowest section ($x = x_m$, say). Suppose that at this section the depth at the deepest point across the channel is D_m and maximum width at this

point is b_m. For rectangular cross-sections D_m is simply the depth and b_m the width. We define

$$(x,y)^* = \frac{(x,y)}{b_m}, \quad z^* = \frac{z}{D_m}, \quad t^* = \frac{t(D_m g')^{\frac{1}{2}}}{b_m},$$

$$(u_i,v_i,w_i)^* = \frac{(u_i,v_i,w_i)}{(D_m g')^{\frac{1}{2}}}, \quad p_i^* = \frac{p_i}{(\rho_i D_m g')}, \quad \rho_i^* = \frac{2\rho_i}{\rho_1+\rho_2}, \tag{1}$$

where the variables with a superscript asterisk are dimensionless and g' is the reduced gravity ($g' = 2g(\rho_1-\rho_2)/(\rho_1+\rho_2)$). Note that the channel depth and width are also non-dimensionalised by D_m and b_m respectively. We shall utilize a right-handed coordinate system with the x-axis along the channel so that the lower layer has a positive velocity and the z-axis is in the vertically upward direction. The subscript i takes the value 1 for the lower layer and 2 for the upper layer.

The shallow-water equations may be written in the form

$$\left.\begin{aligned} &\frac{\partial u_i}{\partial t}+u_i\frac{\partial u_i}{\partial x}+v_i\frac{\partial u_i}{\partial y} = -\frac{\partial}{\partial x}\left(\frac{p_i}{\rho_i}+\frac{z}{\rho_1-\rho_2}\right),\\ &\frac{\partial v_i}{\partial t}+u_i\frac{\partial v_i}{\partial x}+v_i\frac{\partial v_i}{\partial y} = -\frac{\partial}{\partial y}\left(\frac{p_i}{\rho_i}+\frac{z}{\rho_1-\rho_2}\right),\\ &\frac{\partial h_i}{\partial t}+\frac{\partial}{\partial x}(h_i u_i)+\frac{\partial}{\partial y}(h_i v_i) = 0, \end{aligned}\right\} \tag{2}$$

where the superscript asterisks have been dropped and h_1, h_2 are the depths of the lower and upper layers respectively. The momentum equations in (2) may be integrated to yield Bernoulli's equation in the form

$$G_i = \frac{\partial \Phi_i}{\partial t}+\tfrac{1}{2}(u_i^2+v_i^2)+\frac{p_i}{\rho_i}+\frac{z}{\rho_1-\rho_2}, \tag{3}$$

where G_i, $i = 1,2$, are constant. The Bernoulli potential, G_i, is conserved by a material particle and Φ_i is a velocity potential (such that $\boldsymbol{u}_i = \nabla\Phi_i$). Throughout most of this paper our attention will be confined to the final steady state. Thus we set $\partial/\partial t = 0$ in (2) and (3).

As the channel geometry is slowly varying and the flow irrotational, all streamlines are relatively straight in the sense that $u_i \gg v_i$. This allows us to eliminate the pressure between G_1 and G_2 to write

$$\Delta G = G_1-G_2 = \tfrac{1}{2}(u_1^2-u_2^2)+(H+h)\frac{(\rho_1-\rho_2)}{} \tag{4}$$

where $H = H(x,y)$ is the elevation of the channel floor above datum and $h = h(x,y)$ is the thickness of the lower layer. The total depth of the channel is $D = D(x,y)$. Note that we do not restrict the shape of the channel cross-section at this stage. For steady flow the difference ΔG will be constant everywhere (except across regions of dissipation such as hydraulic jumps).

Suppose the lower layer occupies an area $S_1 = S_1(x,h)$ of the cross-section, and the upper layer $S_2 = S_2(x,h)$. From continuity for the layer flow rates (volume fluxes),

$$q_i = S_i u_i, \tag{5}$$

are conserved. Provided that the channel has rigid boundaries, or at least a rigid-lid approximation is valid (external Froude number much smaller than unity), the total cross-sectional area of the channel at a given x,

$$S = S(x) = S_1+S_2, \tag{6}$$

is constant. For true exchange flows ($q_1 q_2 \leqslant 0$) we define the exchange flow rate, $\bar{q}$, as

$$\bar{q} = q_1 - q_2 = |q_1| + |q_2|, \tag{7}$$

and the net barotropic flow rate, Q, as

$$Q = q_1 + q_2 = |q_1| - |q_2|. \tag{8}$$

For the purposes of this study we shall consider $\bar{q}$ as an initially unknown parameter (to be determined) and Q as an independent (prescribed) parameter. The reservoir conditions must be such that the net barotropic flow Q is provided by, for example, a difference in the free-surface heights between the two reservoirs.

3. Information propagation

As with the single-layer counterpart, information is propagated by long, small-amplitude gravity waves; for two-layer flows these waves are on the density interface. By analysing such waves modes in a channel of uniform rectangular cross-section (depth D) with arbitrary velocities in the two layers (relative to a frame of reference fixed with respect to the channel), we may show that the two (dimensional) phase velocities (relative to the same frame of reference) are given by

$$C_1, C_2 = \frac{(D-h)\,u_1 + h u_2}{D} \pm \left\{ \frac{(D-h)\,h}{D} g' \left[1 - \frac{(u_1 - u_2)^2}{D g'} \right] \right\}^{\frac{1}{2}}. \tag{9}$$

(In our dimensionless system (9) holds with g' set to unity.) If C_1 and C_2 are of opposite signs, information is able to propagate in both directions and the flow is said to be *subcritical*. In contrast, if C_1 and C_2 are of the same sign, information about any disturbances is able to propagate in one direction only and the flow is *supercritical*. Note that there are two supercritical states (with the phase velocity vectors pointing towards the left or the right) and only one subcritical state. The necessity for two hydraulic transitions to change from one supercritical state to the other was first recognized by Wood (1968).

The basic character of this information propagation is embodied within the definition of the composite Froude number. Traditionally this is expressed in terms of the dimensional layer Froude numbers as

$$\begin{aligned} F^2 &= F_1^2 + F_2^2, \\ &= \frac{u_1^2}{h_1 g'} + \frac{u_2^2}{h_2 g'}, \end{aligned} \tag{10}$$

which may more usefully be written as

$$F^2 = 1 + \frac{h_1 + h_2}{h_1 h_2 g'} C_1 C_2. \tag{11}$$

Thus the composite Froude number is a measure of whether the flow is subcritical or supercritical, though if the flow is supercritical, it does not give any indication of the direction of information propagation.

Consider the flow through a channel of varying cross-section. Suppose we know Q, $\bar{q}$ and ΔG at some point along the channel. We may trace the solution from this point in both directions for subcritical flows as the small-amplitude waves are able to propagate any changes at this point in both directions. However, if the flow is supercritical, small changes in Q, $\bar{q}$ or ΔG will only be propagated in one direction, and are thus unable to affect the flow in the other direction (unless the waves grow to finite amplitude). Somewhere along the channel there may be a smooth transition

from a subcritical flow to a supercritical flow with both phase velocities away from the subcritical region. Any disturbances will be swept out of the subcritical region. In contrast, the transition to subcritical flow from supercritical flow with both phase velocities towards the subcritical region must be abrupt and take the form of a hydraulic jump; propagation of the slower-moving wave will be reversed on entering the subcritical region. The instability leading to the formation of the jump has been discussed by Pratt (1984) for single-layer flows.

Any subcritical region can therefore be said to *control* the flow provided any bounding supercritical regions have their phase velocities away from the subcritical region. We need consider only processes within subcritical regions of the flow: disturbances elsewhere are unable to propagate against the supercritical flow to influence the subcritical region.

Flows that contain a subcritical region bounded on both sides by appropriate supercritical regions will be termed *fully controlled*. If the flow is supercritical on only one side of the subcritical region, the flow is *partially controlled*. Flows that are subcritical everywhere are not controlled. Note that a hydraulic jump (which violates the basic assumptions) may form within a supercritical region without affecting the controlling subcritical region, provided that the amplitude of the jump is not too large. This provides the mechanism for matching a supercritical flow in the channel to a subcritical flow within the reservoir. We shall return to the restrictions that this imposes on the interface height in the two reservoirs in §7.

Long (1956) analysed the linear stability problem for long-wave disturbances to an inviscid shear flow between two layers bounded by rigid, horizontal plates. In terms of our present non-dimensional notation, he found the flow to be stable if

$$(u_1-u_2)^2 \leqslant D. \tag{12}$$

Noting that the product u_1u_2 is negative for exchange flows, we may replace u_2 with the composite Froude number from (10) and write

$$D|u_1|^2-2D^{\frac{1}{2}}h|u_1|-[D(F^2-1)-F^2h]\,h \leqslant 0. \tag{13}$$

For critical flow $|u_1| \leqslant D^{\frac{1}{2}}$ and $h \in [0,D]$ so (3) shows that the flow is never unstable. Marginal stability ((13) equals zero) may occur if $D^{\frac{1}{2}}u_1 = h$. For $F^2 < 1$, the inequality of (13) holds for all values of u_1 and h, so subcritical flows are always stable with respect to long-wave disturbances. The bounding supercritical flow may be unstable if $D^{\frac{1}{2}}u_1$ lies in the range

$$h \pm [(F^2-1)\,(D-h)h]^{\frac{1}{2}}, \tag{14}$$

though we note that the supercritical nature of the flow may wash such a disturbances a significant distance away from the subcritical region before they have grown to finite amplitude. We may thus consider the subcritical region as stable. Lawrence (1985) has considered in detail the instability in the equivalent problem with the two layers flowing in the same direction.

4. Hydraulic functional

4.1. *Definition*

In his work on single-layer hydraulics, Gill (1977) noted the similarity of a wide class of hydraulic-like problems, and showed that they all had a common mathematical structure. The present two-layer hydraulic problem is no exception, although utilizing Gill's formalism is not as simple as for the single-layer flow.

For two-layer flows we shall formulate a functional J which has the following properties:

(i) Configurations of the interface which satisfy the basic assumptions of conserving the Bernoulli potentials and volume flow rates of the two layers are solutions to

$$J(a_0,a_1,a_2,\ldots,Q,\bar{q},\mathscr{G};h)=0, \tag{15}$$

where the single dependent variable h depends on the along-channel coordinate x only through a set of geometric parameters $a_0,a_1,a_2,\ldots$. We shall treat the net barotropic flow rate Q as a prescribed parameter. The exchange flow rate $\bar{q}$ and constant $\mathscr{G}$ are parameters which select between the various conceivable flows. The constant $\mathscr{G}$ is similar to the constant on the right-hand side of Gill's equation (3.1). The physical significance of $\mathscr{G}$ depends on the form of $J(\cdot\,;h)$ and will be explained shortly.

(ii) The functional $J(\cdot\,;h)$ is multiple valued for some range of $a_0,a_1,a_2,\ldots$ in that there is more than one value of h satisfying (15).

(iii) There is some sort of *constriction* in the sense that at some point along the channel

$$K=\frac{\partial J}{\partial a_0}\frac{\mathrm{d}a_0}{\mathrm{d}x}+\frac{\partial J}{\partial a_1}\frac{\mathrm{d}a_1}{\mathrm{d}x}+\frac{\partial J}{\partial a_2}\frac{\mathrm{d}a_2}{\mathrm{d}x}+\ldots=0. \tag{16}$$

The functional J is a surface in $(a_0,a_1,a_2,\ldots,Q,\bar{q},\mathscr{G},h)$-space. *Control sections* represent the transition from one *sheet* of the surface to another. Different sheets meet along lines defined by

$$\partial J/\partial h=0. \tag{17}$$

Differentiation of (15) with respect to x shows that $(\partial J/\partial h)\,(\mathrm{d}h/\mathrm{d}x)=-K$ along such lines. Unless $K=0$, $\mathrm{d}h/\mathrm{d}x$ will be infinite and the solution will break down. Therefore K must be zero along lines where the solution sheets meet. Further differentiation of (15) demonstrates that $K=0$ must be a constriction rather than an expansion.

The set of functionals fulfilling the requirements for J is infinite; the relevant solutions to $J=0$ describe the same unique flow for a given geometry and net flow, regardless of the form of J, so long as it conserves mass and Bernoulli potential. It is tempting to identify J with the exchange flow rate $\bar{q}$ to allow (17) to be interpreted as the maximal-exchange criterion often used in single-layer hydraulics and suggested by Whitehead, Leetmaa & Knox (1974) for two-layer flows. We note, however, that J should be single valued with respect to its parameters in that, for given $a_0,a_1,a_2,\ldots,Q,\bar{q},\mathscr{G}$ and h, there is only one value of J. Identifying $\bar{q}$ with J introduces some ambiguity through the need to conserve the difference in the Bernoulli potentials (i.e. we would introduce the roots of a quadratic).

As an alternative we propose a hydraulic functional of the form

$$J(a_0,a_1,a_2,\ldots,Q,\bar{q},\mathscr{G};h)=\mathscr{G}-\tfrac{1}{2}(u_1^2-u_2^2)-(H+h). \tag{18}$$

The requirement $J(\cdot\,;h)=0$ is a statement of conservation of the difference of the Bernoulli potentials. Note that we are not able to determine $\mathscr{G}$ from the pressure heads in the reservoirs due to subcritical reservoir conditions requiring the formation of a hydraulic jump from the supercritical flow into the reservoir; the Bernoulli potentials are not conserved across such a jump.

Differentiation of (18) with respect to x gives

$$\begin{aligned}\partial J/\partial x&=\frac{\partial J}{\partial h}\frac{\mathrm{d}h}{\mathrm{d}x},\\ &=-u_1\frac{\partial u_1}{\partial x}+u_2\frac{\partial u_2}{\partial x}-\frac{\partial(H+h)}{\partial x},\end{aligned} \tag{19}$$

which may be compared with the difference between the x-momentum equations for relatively straight flow in the two layers, viz.

$$\frac{\partial}{\partial t}(u_1-u_2)+u_1\frac{\partial u_1}{\partial x}-u_2\frac{\partial u_2}{\partial x}=-\frac{\partial}{\partial x}(H+h), \tag{20}$$

to show that $(\partial J/\partial h)\,(\mathrm{d}h/\mathrm{d}x)$ plays the same role as $(\partial/\partial t)\,(u_1-u_2)$, should this steady flow be disturbed. We may thus replace $(\partial/\partial t)\,(u_1-u_2)$ in (20) with $(\partial J/\partial h)\,(\mathrm{d}h/\mathrm{d}x)$. The velocity gradients may be eliminated using the continuity equations. For small-amplitude travelling wave solutions we may write $\partial/\partial t=-C_n\,\partial/\partial x$, where C_n, $n=1,2$, are the two phase velocities of such a wave, and so obtain the relationship between the phase velocity of small-amplitude gravity waves (relative to the channel) and the slope $\partial J/\partial h$ of the hydraulic functional, viz.

$$(D-h)\,h\frac{\partial J}{\partial h}\frac{\partial h}{\partial x}-C_n[(D-h)\,u_1+hu_2]\frac{\partial h}{\partial x}+DC_n^2\frac{\partial h}{\partial x}=0. \tag{21}$$

From the quadratic form of (21) we may determine the product of the two phase velocities, C_1C_2, and utilize (11) to show the composite Froude number is related to the hydraulic functional by

$$F^2=1+\frac{\partial J}{\partial h}. \tag{22}$$

Thus the transition from one solution sheet to another corresponds to critical conditions ($F^2=1$).

The direction of the phase velocities is given by the second term of (21) as

$$D(C_1+C_2)=(D-h)u_1+hu_2. \tag{23}$$

The numerically larger phase velocity will be in the same direction as the thinner, faster moving layer. For non-trivial solutions to (21) we may eliminate the $\partial h/\partial x$ terms and then differentiate the expression with respect to h to show that if both $\partial J/\partial h=0$ and $\partial^2 J/\partial h^2=0$ then both phase velocities vanish.

For given x, Q, $\bar{q}$ and $\mathscr{G}$ there will, in general, be three solutions to $J(\cdot\,;h)=0$ with real h. Two of these solutions will be supercritical ($\partial J/\partial h>0$) and one subcritical ($\partial J/\partial h<0$). The supercritical root with a value of h falling below the value for the subcritical root will have its phase velocities towards the left; the other supercritical root with h larger than that for the subcritical root will have its phase velocities towards the right. We shall distinguish these two supercritical roots as the *left-directed* and *right-directed* supercritical flows.

Cross-channel variations in channel depth do not affect any of the above arguments. Thus this functional formulation may be applied to a channel of arbitrary cross-section (provided that the interface is continuous). Moreover, provided the flow remains relatively straight, cross-channel variations in the interface height and layer velocities (e.g. flows which are not irrotational or flows in rotating channels) can fit within this framework: the constant $\mathscr{G}$ may be a function of y (we only require $\partial\mathscr{G}/\partial x=0$).

4.2 *Rectangular cross-section*

For the remainder of this paper we shall confine our attention to the flow through channels of rectangular cross-section. Figure 1 shows the typical geometry for such a channel. In our dimensionless system the channel depth D and width b are both

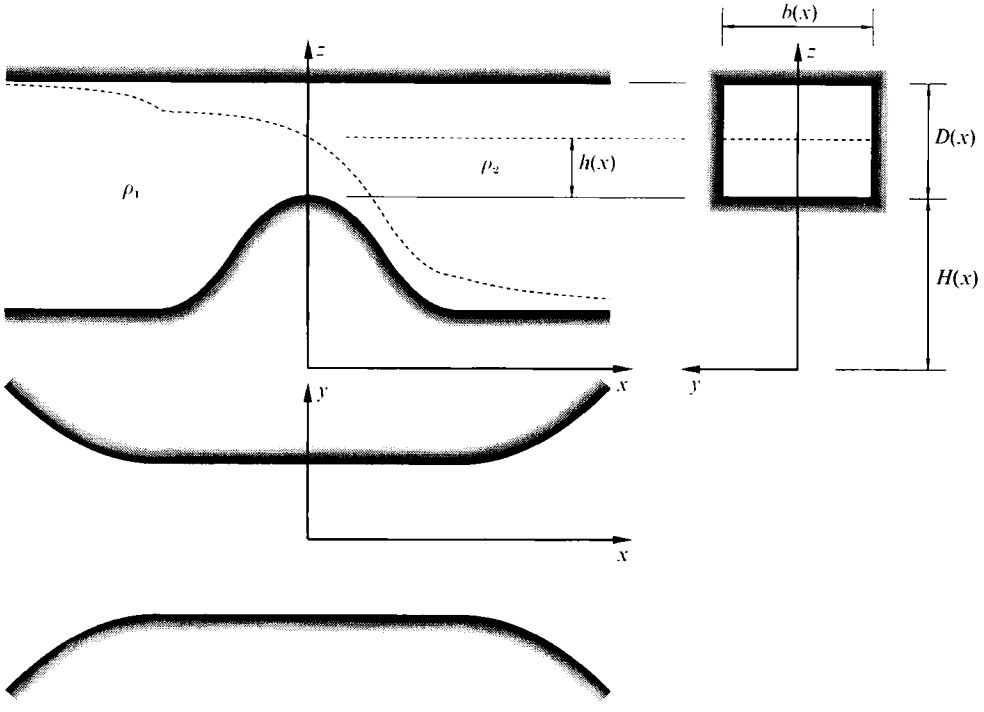

FIGURE 1. Definition sketch of a channel with a rectangular cross-section.

unity at the shallowest section. For convenience we shall write the height of the interface above the channel bottom as

$$h(x) = (\tfrac{1}{2}+A(x))\,D(x), \tag{24}$$

and note that $\partial/\partial h = D^{-1}\partial/\partial A$. We shall call the dependent variable $A = A(x)$ the *interface height coefficient*.

The sectional areas, S_1 and S_2, occupied by the two layers are simply

$$S_1 = Db(\tfrac{1}{2}+A), \quad S_2 = Db(\tfrac{1}{2}-A). \tag{25}$$

Eliminating u_1 and u_2 from (18) using (5)–(8) and (25) enables us to write

$$J(\cdot\,;A) = \mathscr{G}+\left[\frac{1}{2Db}\right]^2 \frac{A(\bar{q}^2+Q^2)-2(\frac{1}{4}+A^2)\,Q\bar{q}}{(\frac{1}{4}-A^2)^2} - H - D(\tfrac{1}{2}+A), \tag{26}$$

and its derivative with respect to A as

$$\frac{\partial J}{\partial A} = \left[\frac{1}{2Db}\right]^2 \frac{(\frac{1}{4}+3A^2)(\bar{q}^2+Q^2)-A(3+4A^2)\,Q\bar{q}-4D^3b^2(\frac{1}{4}-A^2)^3}{(\frac{1}{4}-A^2)^3}. \tag{27}$$

If the position of one control section is $x = x_c$, say, and the interface height coefficient at this section is $A = A_c$, then we solve $\partial J/\partial A = 0$ (i.e. critical conditions) from (27) to show that the exchange flow rate is given by

$$\bar{q}_{\text{crit}} = \frac{-a_1+(a_1^2-4a_0a_2)^{\frac{1}{2}}}{2a_2} \tag{28a}$$

where

$$a_2 = \tfrac{1}{4}+3A^2, \quad a_1 = -A(3+4A^2)Q, \quad a_0 = (\tfrac{1}{4}+3A^2)Q^2-4D^3b^2(\tfrac{1}{4}-A^2)^3. \tag{28b}$$

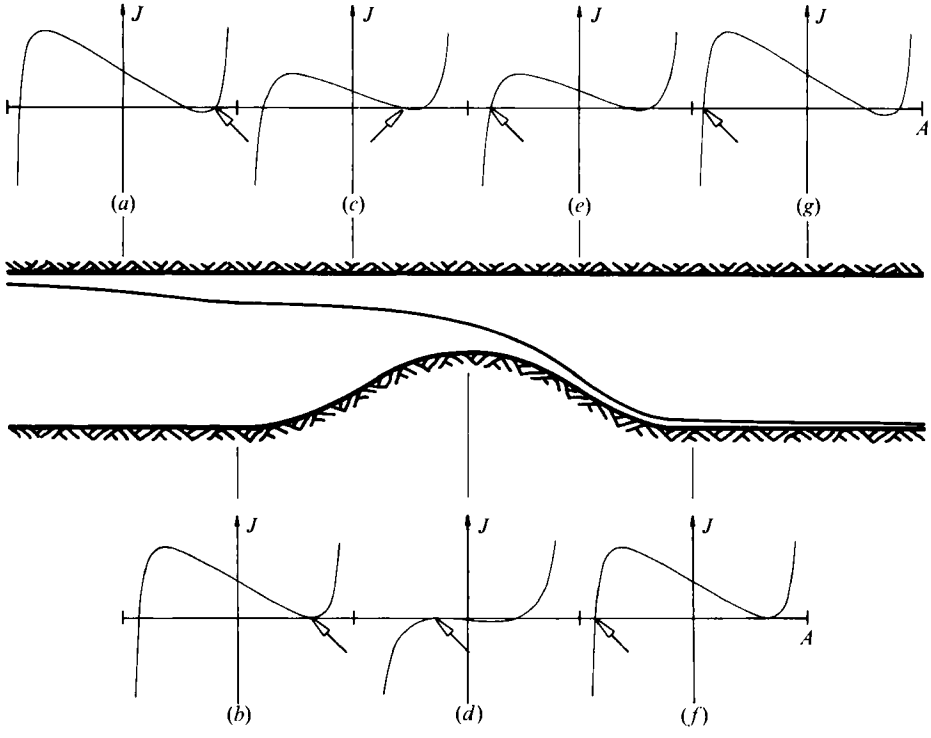

FIGURE 2. Variations in the hydraulic functional for a fully controlled flow over a simple sill. The interface profile along the channel is shown, along with plots of the hydraulic functional at seven locations along the channel. For each plot of the functional the A-axis goes from $-\frac{1}{2}$ to $\frac{1}{2}$. The root of $J = 0$ giving the interface position shown is indicated by an arrow. Plots of J at sections (a) and (g) are identical owing to identical geometry, although the indicated root differs. Similarly for sections (b) and (f), and (c) and (e). The two controls are positioned at sections (b) and (d).

The values of D, b and A are those for $x = x_c$. The subscript crit indicates that the exchange flow rate gives critical conditions at the section. The constant $\mathscr{G}$ may then be evaluated from $J = 0$.

4.3. *Features*

Figure 2 sketches how the hydraulic functional may vary along a channel containing a simple sill. The supercritical regions to either side of the sill allow matching on to the conditions within the reservoirs by means of hydraulic jumps; for the time being we shall ignore these jumps and concentrate on the region of flow where all the basic assumptions hold.

At section (a), near the dense reservoir, the interface is close to the top of the channel. The hydraulic functional for this section is plotted above the channel; the appropriate root to $J = 0$ is indicated by an arrow. Moving towards the base of the sill the form of the hydraulic functional changes in response to the geometry. The left-directed supercritical ($\partial J/\partial A > 0$) root of $J = 0$ (value of A larger than the subcritical root) moves towards smaller values of A and closer to the subcritical root ($\partial J/\partial A < 0$). At section ($b$) (plotted below the channel) the subcritical and supercritical roots coincide giving critical conditions ($\partial J/\partial A = 0$). The double root allows the flow to pass from a supercritical branch to a subcritical branch of the solution. The non-zero phase velocity remains directed towards the left. Moving on towards the crest of the sill, the continued change in the geometry forces the two

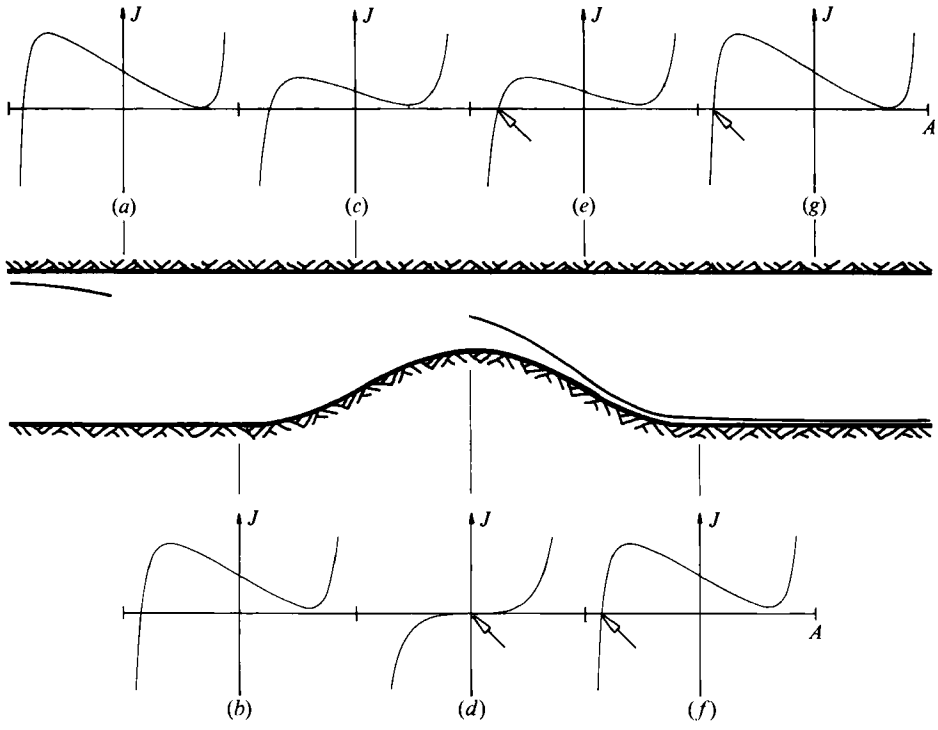

FIGURE 3. Variations in the hydraulic functional for an unrealizable flow over a simple sill. The calculation assumed that both controls were positioned at the sill crest (section d). The channel geometry is identical to that for figure 2. Again the A-axis ranges from $-\frac{1}{2}$ to $\frac{1}{2}$ for each plot of the functional.

roots apart once more. At section (c) the flow is subcritical, the root moving closer to the second supercritical solution as shown on the appropriate plot above the channel. The sill crest (section d) sees the subcritical root and the right-directed supercritical roots coincide. The flow is able to undergo a second hydraulic transition, allowing it to follow the right-directed supercritical root onward towards the light reservoir.

The geometry at section (e) is identical to that at (c) and so the hydraulic functional takes the same form. The flow, however, now corresponds to the supercritical root with both phase velocities towards the light reservoir. Moving out into the light reservoir at positions (f) and (g) the relevant roots of $J = 0$ remain distinct, even though $J = 0$ has a double root at section (f). The flow is not able to undergo any further hydraulic transitions.

The important feature to note is that the interface height progresses smoothly along the channel from one supercritical root at the dense-reservoir end of the channel, to the other supercritical root at the light-reservoir end of the channel; the flow is fully controlled with two hydraulic transitions.

Figure 3 plots the hydraulic functional for the same channel as figure 2 but assumes that the two control sections coincide at the crest of the sill (the values of $\bar{q}$ and $\mathscr{G}$ differ from those of figure 2). While there is no difficulty tracing the right-directed supercritical solution from the sill crest towards the light reservoir, we are unable to trace the solution towards the dense reservoir as two of the roots to $J = 0$ become complex. The remaining supercritical root has both phase velocities

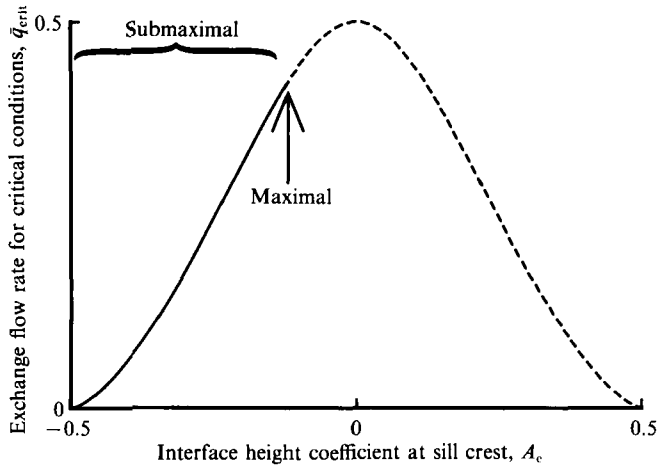

FIGURE 4. The exchange flow rate required to produce critical conditions at the sill crest ($\bar{q}_{crit}$; geometry as for figures 2 and 3) as a function of the interface height coefficient (A_c) at that point. The dashed part of the curve indicates configurations that cannot be traced towards the dense reservoir.

towards the right of figure 3 and represents an unrealizable flow to the left of the sill crest due to critical conditions at the crest (see sections *a–c*). Note, however, that in the expanding region towards the dense reservoir $J = 0$ regains three real roots. Thus if we were to look only at the sill crest and in the dense reservoir we would miss the inability for the flow to be traced.

In figure 4 we plot how the exchange flow rate varies as a function of A at the sill crest for all flows having critical conditions at this point and no net flow along the channel (plots for $Q \neq 0$ have a similar form with a single turning point though are skewed away from symmetry about $A = 0$). The curve is simply the solution $\bar{q} = \bar{q}_{crit}$ to $\partial J/\partial A = 0$ at the sill crest ($x = x_c$). Notice that critical conditions with $A_c = A(x = x_c) = 0$ yields the largest value of $\bar{q}_{crit}$; however, as we have demonstrated, such a flow cannot be connected to the dense reservoir when a sill is present in the channel. The dashed portion of the curve is figure 4 indicates values of A_c that cannot be connected to the reservoirs for a channel with the geometry of figures 2 and 3; the solid part of the curve indicates values that can be traced towards both reservoirs.

Fully controlled solutions correspond to the boundary of these two regions; if the value of A at the sill crest is any larger than that associated with the local minimum in $J(\cdot\,; A)$ then this turning point will rise above the A-axis at some location along the channel, leaving only one real solution (such as in figure 3). On the other hand, if the value of A at the sill crest is less than that at the boundary of these two regions, the local minimum will never be a solution to $J(\cdot\,; A) = 0$ and so the flow will not be able switch to the left-directed supercritical solution. Such flows are partially controlled (the flow is subcritical everywhere to the left of the sill crest) and may be considered *submaximal* in that they yield a lower value of $\bar{q}_{crit}$ than the fully controlled solution. The fully controlled flow is *maximal* in the sense that it yields the largest exchange flow rate of any realizable flow. We shall delay further discussion on submaximal or partially controlled solutions until §7.

The problem is how to determine the values of $\bar{q}$ and $\mathscr{G}$ so that the solution is traceable and able to be matched onto the conditions in both reservoirs. For fully controlled solutions we must determine the boundary between realizable and unrealizable flows. Searching over the full $(\bar{q}, \mathscr{G})$ space and tracing the solution along

the channel for each pair of $\bar{q}$ and $\mathscr{G}$ would be prohibitive from a computational standpoint. In the next sub-section we shall present an alternative approach to this problem.

4.4 *Solution process*

Flows which are not controlled are of little interest as they represent identical conditions in the two reservoirs. Partial control allows the conditions within the two reservoirs to differ through a single hydraulic transition and the possibility of a hydraulic jump in one reservoir. Solution is straightforward: the subcritical flow must be matched onto the appropriate reservoir; critical conditions then occur at some appropriate point along the channel. For the following two sections we shall focus our attention on the more interesting case of fully controlled flows.

The aim of the solution process is to determine the quantities $\bar{q}$ and $\mathscr{G}$ yielding a continuous solution which may be traced from a supercritical flow into the dense reservoir, through two hydraulic transitions (one either side of a region of subcritical flow; this region may be vanishingly small) and into a supercritical region leading towards the light reservoir. Rather than searching the entire $(\bar{q}, \mathscr{G})$ space, determining the values of $\bar{q}$ and $\mathscr{G}$ that fulfill the necessary criteria, it proves more convenient to search for the location of the two controls, utilizing (16) to give some indication of where to look.

Consider a channel with the controls positioned at $x = x_c$ and $x = x_v$. Suppose the position x_c is known. By assuming the other control is at $x = x_a$, say, and requiring $J(\cdot\,; A) = 0$ and $\partial J/\partial A = 0$ at both sections, we may determine the exchange flow rate required to give critical conditions at both x_c and x_a, ignoring the geometry in the remainder of the channel. The constant $\mathscr{G}$ may be obtained simply from $J = 0$. If we were now to trace this solution along the channel, we would discover that there would only be one real root to $J = 0$ in the neighbourhood of $x = x_v$. This root is supercritical with both phase velocities towards x_c. This is an unstable situation as the slower moving long wave at x_v would come to rest at x_c.

The closer x_a is to x_v the smaller the range of x over which there is only one real root. When $x_a = x_v$ three real roots exist everywhere, though two (or all three) of them coincide at x_c and x_v. The flow is on the boundary between realizable and unrealizable solutions to $J(\cdot\,; A) = 0$. The sections x_c and x_v represent saddle points for the functional J: $\partial J/\partial A = 0$ and the constriction condition (equation (16)) which may be written as

$$K = \frac{\partial J}{\partial D}\frac{\mathrm{d}D}{\mathrm{d}x} + \frac{\partial J}{\partial H}\frac{\mathrm{d}H}{\mathrm{d}x} + \frac{\partial J}{\partial b}\frac{\mathrm{d}b}{\mathrm{d}x} = 0. \tag{29}$$

In addition the solution with $x_a = x_v$ yields the lowest exchange flow rate for any pair of (x_c, x_a) producing critical conditions at both x_c and x_a (without necessarily requiring the flow to exist elsewhere in the channel). We may prove this by considering how the functional at $x = x_a$ responds to small changes in x_a. Suppose one control is fixed at $x = x_c$ (say) and the other at $x = x_a$ perturbed slightly from its original location. The functional at $x = x_a$ responds as

$$\left.\frac{\mathrm{d}J}{\mathrm{d}x}\right|_{x=x_a} = \frac{\partial J}{\partial D}\frac{\mathrm{d}D}{\mathrm{d}x_a} + \frac{\partial J}{\partial H}\frac{\mathrm{d}H}{\mathrm{d}x_a} + \frac{\partial J}{\partial b}\frac{\mathrm{d}b}{\mathrm{d}x_a} + \frac{\partial J}{\partial A}\frac{\mathrm{d}A}{\mathrm{d}x_a} + \frac{\partial J}{\partial \bar{q}}\frac{\mathrm{d}\bar{q}}{\mathrm{d}x_a} + \frac{\partial J}{\partial \mathscr{G}}\frac{\mathrm{d}\mathscr{G}}{\mathrm{d}x_a}, \tag{30}$$

which must vanish for the solution to $J(\cdot\,; A) = 0$ to be maintained at $x = x_a$. We may eliminate the final term of (30), using the comparable expression at $x = x_c$. Since the flow is critical at $x = x_a$ we may put $\partial J/\partial A = 0$. The first three terms of (30) must

vanish to satisfy the constriction condition (29) (this is effectively a statement that the flow must be realizable), reducing the expression to

$$\left[\left.\frac{\partial J}{\partial \bar{q}}\right|_{x=x_a} - \left.\frac{\partial J}{\partial \bar{q}}\right|_{x=x_c}\right]\frac{\mathrm{d}\bar{q}}{\mathrm{d}x_a} = 0. \tag{31}$$

In general the dependence of J on $\bar{q}$ will be different at x_c and x_a, so $\mathrm{d}\bar{q}/\mathrm{d}x_a$ must vanish. The exchange flow rate is therefore a stationary point with respect to the location of the control x_a. The second derivative $\mathrm{d}^2J/\mathrm{d}x^2$ may be used to show that the realized exchange flow rate is the minimum. Repeating the analysis with x_a and x_c interchanged completes the proof.

The realized exchange flow rate is a saddle point: fully controlled flow is maximal in the sense that a lower value of $\bar{q}$ corresponds to partial control, and minimal in the sense that critical conditions at x_c and x_v yield a lower value of $\bar{q}$ than critical conditions at any other pair sections (if the intervening geometry is ignored).

Below we give an outline of an algorithm which may be used to determine the fully controlled flow through any arbitrary along-channel geometry.

(i) Guess the position of one of the control sections, $x = x_c$ (say). Frequently this will represent some geometric constriction in the channel (see later in this section).

(ii) Determine $A_{max}(x = x_c)$, the interface height which maximizes $\bar{q}_{crit}(x = x_c)$ (equation (28) with $A = A_c$ and the geometry set for $x = x_c$).

(iii) Guess the position of the second control section, x_v. This need not be at a geometric feature in the channel.

(iv) Determine $A_{max}(x = x_v)$.

(v) Guess the interface height A_c at $x = x_c$. If x_v is closer to the dense reservoir than x_c then A_c must be less than $A_{max}(x = x_c)$. If x_v is closer to the light reservoir, then $A_c > A_{max}(x = x_c)$.

(vi) Calculate the critical exchange flow rate $\bar{q}_c = \bar{q}_{crit}(A = A_c)$ and the value of $\mathscr{G}$ to give $J(\cdot\,; A_c) = 0$.

(vii) If x_v is closer to the dense reservoir than x_c then find the turning point $\partial J/\partial A = 0$ at $x = x_v$ with $A > A_{max}(x = x_v)$, otherwise the turning point with $A < A_{max}(x = x_v)$.

(viii) Determine the value $J_v = J(x = x_v)$ for the turning point calculated in step (vii).

(ix) If $J(\cdot\,; A_v) = 0$ then go to step (x); if not, adjust A_c and return to step (vi).

(x) If $\bar{q}_c$, evaluated in step (vi), is the minimum for all values of x_v then go to step (xi); if not, adjust x_v and return to step (iv).

(xi) If $\bar{q}_c$ is the minimum for all values of x_c then stop; if not, adjust x_c and return to step (ii).

For a large variety of channels the constriction equation (29) may be utilized to give some indication of the position of the control sections. If $\mathrm{d}D/\mathrm{d}x$, $\mathrm{d}H/\mathrm{d}x$ and $\mathrm{d}b/\mathrm{d}x$ all vanish simultaneously, and are minimum values at a particular section, then one of the controls – the *primary* control x_c – is at this section. The relatively simple along-channel geometries of this paper fall in this category with one control section always located at the crest of the sill, and so steps (i) and (xi) may be omitted. If the minima in channel depth and width do not coincide, it is still likely that a control section will be positioned at one or the other or both of these geometric constrictions, simplifying the search associated with step (xi).

The position of the second or *virtual* control may be more difficult to find. For some channels it will be at a second stationary point in the geometry. Alternatively, if

there is a net barotropic flow through the channel, the virtual control may be positioned upstream, with respect to the net flow, of the primary control in a region of channel possessing no geometric constriction. Under these circumstances it is a combination of the geometric $\mathrm{d}\cdot/\mathrm{d}x$ and $\partial J/\partial\cdot$ terms in (29) which give the functional a constriction.

Our nomenclature, primary and virtual controls, has been introduced to ease the identification of the mechanisms positioning the two controls. The primary control will be positioned at some geometric constriction; for all channels dealt with in this paper it will be positioned at the sill crest. The virtual control may be positioned at some secondary geometric constriction, in which case it will be called an *exit* or *foot* control, or at some other point along the channel which has no remarkable geometric features.

Differentiation of (27) with respect to A shows that, for critical conditions, $\partial\bar{q}/\partial A$ vanishes when $\partial^2 J/\partial A^2 = 0$. Thus $A_{\max}$ corresponds to the three roots of $J(\cdot\,;A) = 0$ coinciding. Furthermore, at a given section the turning points in J must lie on opposite sides of $A_{\max}$, regardless of the values of $\bar{q}$ and $\mathscr{G}$. It is straightforward to show that

$$A_{\max} = Q/(2D^{\frac{3}{2}}b). \tag{32}$$

In the next section we shall apply the hydraulic formulation to flows through channels of constant depth.

5. Channels of constant depth

Channels of rectangular cross-section with a constant depth (and bottom elevation: $H = 1-D$, say) but varying width are the most straightforward to analyse and have been studied by Armi (1986) and Armi & Farmer (1986). The purpose of this section is to illustrate and confirm the present functional approach using this well-known problem.

As along-channel lengthscales are of no importance (i.e. provided they are much greater than the width or depth), we can consider the geometry as symmetric about the narrowest section ($x = 0$, say). If there is no net flow along the channel, we could appeal to this symmetry to show that the controlled flow must be antisymmetric with both controls coinciding at the contraction (the narrowest section). We shall show how this fits in with the functional approach before looking at the effect of a net flow.

When the channel depth and bottom elevation are constant, the constriction equation (29) reduces to

$$K = \frac{\partial J}{\partial b}\frac{\mathrm{d}b}{\mathrm{d}x}, \tag{33}$$

which vanishes when $\mathrm{d}b/\mathrm{d}x = 0$ (the contraction) and/or

$$\frac{\partial J}{\partial b} = \frac{-1}{2D^2b^3}\frac{A(\bar{q}^2+Q^2)-2(\frac{1}{4}+A^2)Q\bar{q}}{(\frac{1}{4}-A^2)^2} = 0. \tag{34}$$

In the absence of net forcing ($Q = 0$) the condition in (34) requires $A = 0$. Suppose for the moment that the controls are both positioned at $x = x_{\mathrm{a}}$. We know that the controls must coincide as $\partial J/\partial b = 0$ requires $A = A_{\mathrm{a}} = A_{\max} = 0$, which represents a triple root of $J = 0$. Setting $A = 0$ in (28) and the geometry to that of section x_{a}, we may show that the exchange flow rate associated with this position of the two controls is

$$\bar{q}_{\mathrm{a}} = \tfrac{1}{2}D_{\mathrm{a}}^{\frac{3}{2}}b_{\mathrm{a}}. \tag{35}$$

For the exchange flow rate to be minimized (with respect to the position of the controls), (35) clearly requires the controls to be at the contraction. We may demonstrate the need to minimize $\bar{q}$ by considering the behaviour of the turning points in J. Setting (27) to zero and utilizing (35) allows us to show that turning points in J are located where A is a solution of

$$A^6 - \tfrac{1}{3}A^4 + (3/16)(1+\gamma)A^2 - (1/64)(1-\gamma) = 0, \tag{36}$$

and $\gamma = (b_a/b)^2$. Differentiation of (36) with respect to γ shows that these turning points shift with the channel width ratio as

$$\frac{\partial A^2}{\partial \gamma} = -\frac{3}{4}\frac{12A^2+1}{144A^4 - 32A^2 + 9(1+\gamma)}. \tag{37}$$

Now at $x = x_a$, $A = 0$ and $\gamma = 1$ so $\partial A^2/\partial\gamma = -\frac{1}{24}$. Thus if γ were to increase (i.e. b become less than b_a) away from the control, turning points in J would cease to exist ($A^2 < 0$). To complete the proof we note that a complete solution of (21) with no turning points yields imaginary phase velocities (the real part vanishes) and so the flow is unstable with the instabilities unable to propagate away. Thus the controls must be positioned at the contraction so that γ is never greater than unity.

The introduction of a net barotropic flow through the channel breaks the inherent symmetry, and so we no longer expect both controls to be at the contraction. The primary control remains fixed at the contraction $\mathrm{d}b/\mathrm{d}x = 0$, while the position of the virtual control is set by the $\partial J/\partial b$ vanishing in (34). Solving for A, noting that A must remain finite as $Q \to 0$, we find the relevant solution is $A = A_s$ where

$$A_s = \tfrac{1}{2}Q/\bar{q}. \tag{38}$$

Note that (38) is independent of x. Thus we are able to assert that at $x = x_c = 0$ (the primary control at the contraction) there is a supercritical root with $A = A_s$ in addition to the critical root with $A = A_c$. Solving $J(A = A_s) = 0$, $J(A = A_c) = 0$ and $\partial J/\partial A(A = A_c) = 0$ simultaneously allows us to determine A_c, $\mathscr{G}$ and $\bar{q}$. Subsequent solution of $\partial J/\partial A = 0$ (with $A = A_s$) for the geometry at the virtual control will give us the position of the virtual control. Since $|A_s|$ is greater than $|A_{max}|$ of (32) (they both take the same sign), the virtual control will always be positioned upstream, with respect to the net flow, of the primary control. At the contraction A_c must therefore be closer to zero than A_{max}, though will also take the same sign as A_{max}.

As the net forcing is increased, both $|A_c|$ and $|A_v|$ will increase. Eventually $|Q|$ will reach some value $|Q| = |Q_t| \leqslant D^{\frac{3}{2}}b_c$ for which $|A_v| = \frac{1}{2}$ and the corresponding layer vanishes. Solving the necessary equations ($|Q| = \bar{q}$ alongside $J(\cdot\,; A) = 0$ and critical conditions at the contraction) reveals that

$$|Q_t| = (\tfrac{2}{3}D)^{\frac{3}{2}}b_c, \tag{39}$$

at which point $|A_c| = \frac{1}{6}$ and $b_v \to \infty$. If the strength of the net forcing is increased any further, the virtual control disappears and the flow becomes a single-layer flow with an overlying ($Q > 0$) or underlying ($Q < 0$) passive layer. The unique control is at the contraction, where the interface is related to the net flow by

$$Q^2 = D^{\frac{3}{2}}b_c(\tfrac{1}{2} + |A_c|)^3. \tag{40}$$

The flow is subcritical upstream and supercritical downstream of this point. If $|Q|$ increases past $D^{\frac{3}{2}}b_c$ the flow is simply that through a duct (Armi & Farmer 1986) on the upstream side of the contraction, though it may regain a passive second layer downstream of the contraction.

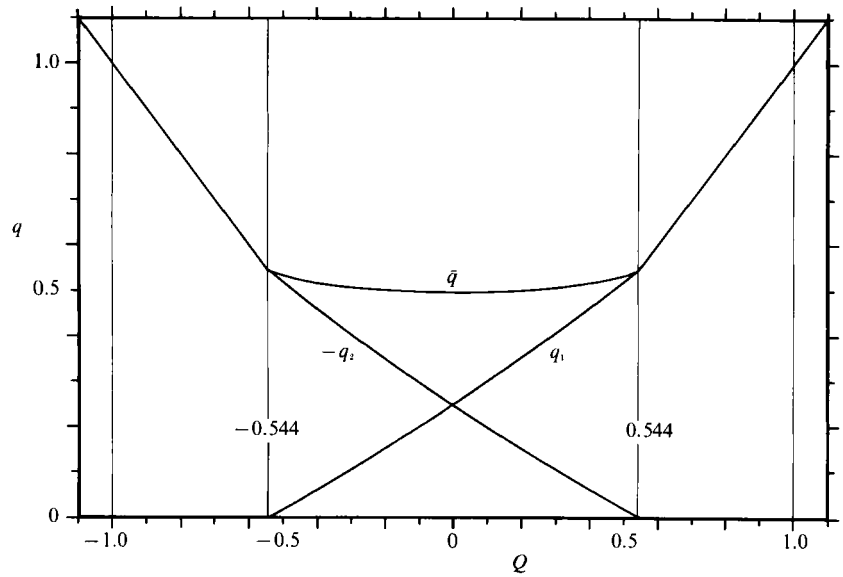

FIGURE 5. The effect of net barotropic forcing on the flow rates through a channel of constant depth.

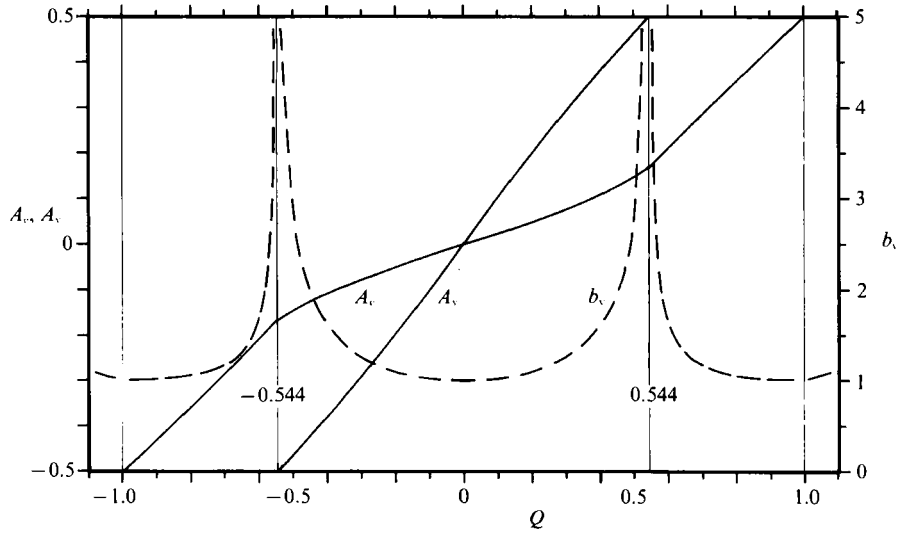

FIGURE 6. The effect of net barotropic forcing (Q) on the flow through a channel of constant depth. Interface height coefficients at the contraction (A_c) and virtual control (A_v) are plotted as solid lines. The dashed line is the width at the virtual control (b_v) for $|Q| < (\frac{2}{3})^{\frac{3}{2}}$, and the width of the front after stagnation of one layer when $|Q| > (\frac{2}{3})^{\frac{3}{2}}$.

Figures 5 and 6 show how the flow through this channel ($D = D_c = 1$ and $b_c = 1$ from our non-dimensionalization) varies as a result of net barotropic forcing. Notice in figure 5 the vanishing of q_1 for $Q < -0.5443$ (i.e. $-(\frac{2}{3})^{\frac{3}{2}}$), and of q_2 for $Q > 0.5443$. This corresponds to $b_v \to \infty$, $|A_c| \to \pm\frac{1}{6}$ and $|A_v| \to \pm\frac{1}{2}$ in figure 6.

These results are identical to those obtained by Armi & Farmer (1986) using a Froude-number-plane formulation of the problem. The advantages of the functional

approach do not become apparent until we consider more complex geometries, such as the flow over a simple sill of arbitrary height; this problem is analysed in the next section.

6. Simple sills

6.1. *No net flow*

As pointed out by Armi (1986) and subsequently Farmer & Armi (1986), two-layer flow over a sill rising from infinite depth differs in a fundamental manner from flow through a contraction in width. The asymmetry of the basic geometry does not allow antisymmetric solutions. The geometry we shall use for this and the following section is outlined in figure 7. In such a geometry, variations in the channel depth are felt more strongly by the lower layer than the upper layer. The geometry presented here differs from that of Armi (1986) and Farmer & Armi (1986) in that the depth away from the sill crest, where the channel begins to increase in width, is finite (cf. Armi 1986, and Farmer & Armi 1986, had $D_w = \infty$). It is important to consider sills rising from finite depths (D_w) in order to understand when the limits of the constant-depth channel and the sill rising from infinite depth may be applied, and to appreciate fully the physical differences between channels of constant depth and sills. Moreover, a number of important features of the flow are missed if only the limits are considered.

The x-scale is included in figure 7 as a means of identifying the various geometric features. As with all steady hydraulic problems, the along-channel lengthscale enters the problem only parametrically through the variations in geometry.

In the absence of net barotropic flow a naïve application of the *maximal exchange* hypothesis would require both controls at the sill crest with $A = 0$. In §4.3 we showed that while it is possible to trace such a solution towards the light reservoir, any attempt to do so towards the dense reservoir fails as the subcritical and appropriate supercritical roots vanish.

The constriction requirement for this channel may be written as

$$K = \frac{\partial J}{\partial b}\frac{\mathrm{d}b}{\mathrm{d}x} + \frac{\partial J}{\partial D}\frac{\mathrm{d}D}{\mathrm{d}x} - \frac{\partial J}{\partial H}\frac{\mathrm{d}D}{\mathrm{d}x} = 0, \tag{41}$$

since $H = \text{const} - D$. Notice that both $\mathrm{d}b/\mathrm{d}x$ and $\mathrm{d}D/\mathrm{d}x$ vanish at $x = -1, 0, 1$, so these three locations are prime candidates for hydraulic control. When $|x| > 1$, $\mathrm{d}D/\mathrm{d}x$ vanishes although $\mathrm{d}b/\mathrm{d}x$ remains non-zero, and so any further controls in these regions would be due to $\partial J/\partial b = 0$.

First consider channels with no net flow ($Q = 0$). We showed in the previous section that $\partial J/\partial b = 0$ is unable to introduce any controls away from the section with smallest $D^{\frac{3}{2}}b$ if $Q = 0$, thus there will not be any controls outside the region $x \in [-1, 1]$. For $0 < |x| < 1$ to give a control, (41) may be applied to (26) giving

$$\frac{\partial J}{\partial D} - \frac{\partial J}{\partial H} = \frac{-A}{2D^3b^2(\frac{1}{4}-A^2)^2}\bar{q}^2 - (\tfrac{1}{2}-A) = 0. \tag{42}$$

Eliminating $\bar{q}^2$ from (42) using (28) yields a quadratic in A with no real roots. Hence (42) has no real roots. Thus there are only six possible combinations of the positions of the control sections, namely

$$(x_c, x_v) \in \{(0,0), (0,-1), (-1,-1), (-1,1), (1,1)\}. \tag{43}$$

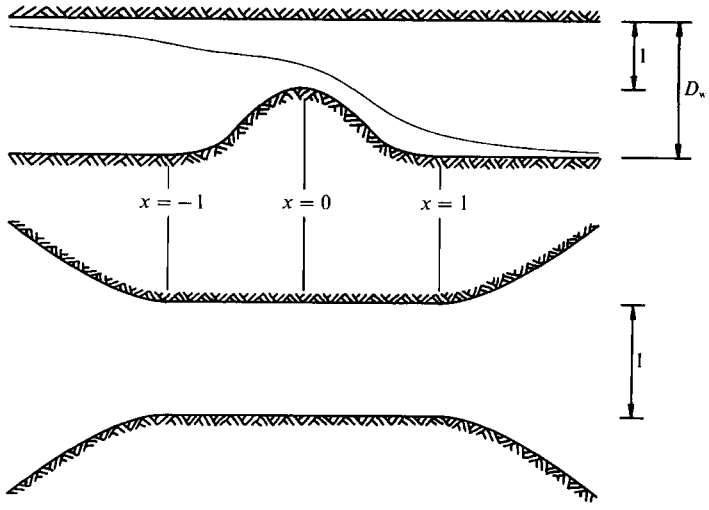

FIGURE 7. Schematic diagram of a simple sill. Top: elevation; bottom: plan view.

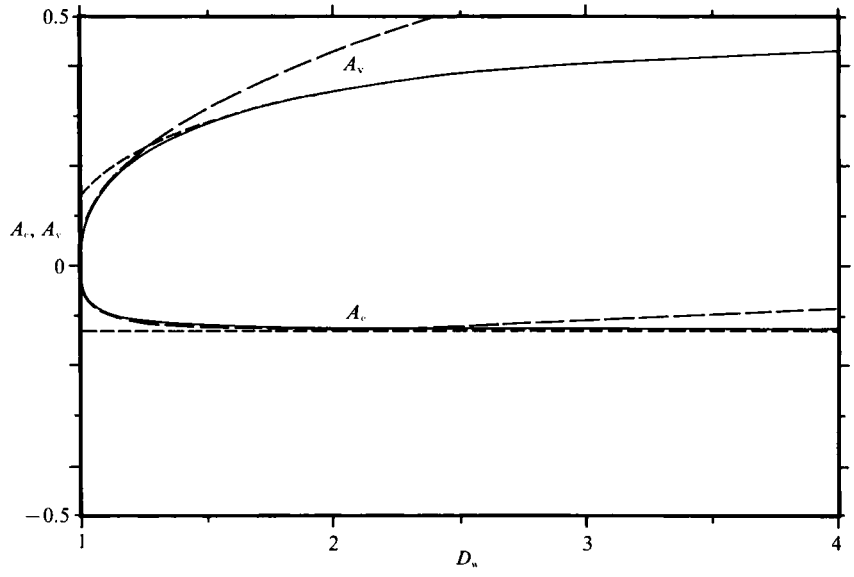

FIGURE 8. Interface height coefficients at the sill crest (A_c) and the virtual (foot) control (A_v) as a function of the channel depth away from the sill (D_w). Solid lines indicate the exact solution; long dashes the $D_w \to 1$ asymptotic expansion; short dashes the $D_w \to \infty$ asymptotic expansion.

Some of these may be eliminated immediately: the $(0,0)$ solution has been shown to be invalid (§4.3), while the $(-1,-1)$, $(-1,1)$ and $(1,1)$ solutions are equivalent, all with a greater total depth (and hence $\bar{q}$) than the $(0,0)$ solution.

The two remaining solutions differ through the need for the interface to slope down towards the lighter reservoir. The primary control is given by $x_c = 0$. If $x_v = -1$ then $A_v > 0$, while $x_v = 1$ would reverse the inequality. Unfortunately it is not possible obtain an explicit solution for A_c and A_v for arbitrary value of D_w. We are, however, able to determine the behaviour in the limits $D_w \to D_c = 1$ and $D_w \to \infty$.

In the $D_w \to 1$ limit we put

$$D_w = 1 + \epsilon^3, \tag{44}$$

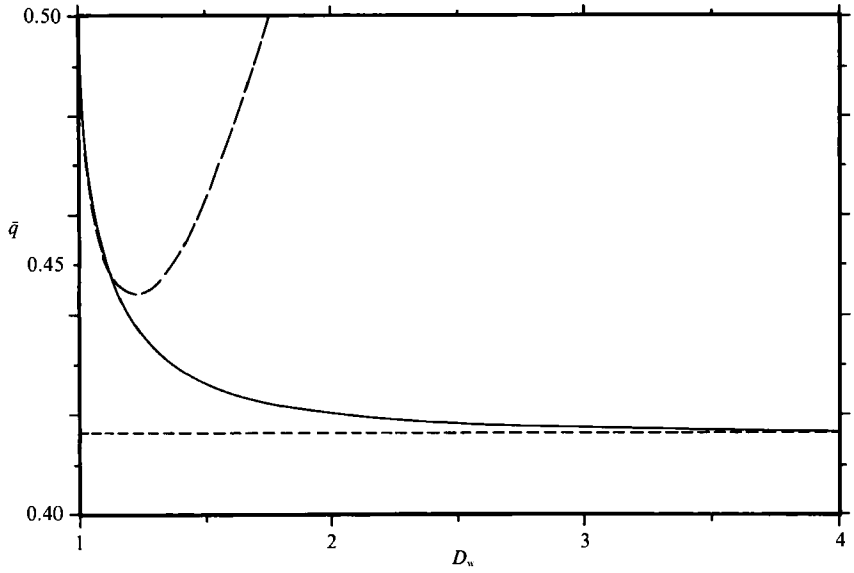

FIGURE 9. Variations in the exchange flow rate over a simple sill as a function of the channel depth away from the sill (D_w). The solid line indicates the exact solution; long dashes the $D_w \to 1$ asymptotic expansion; short dashes the $D_w \to \infty$ asymptotic expansion.

with $\epsilon \to 0$, and find

$$\left.\begin{aligned} A_c &\sim -\tfrac{1}{4}\epsilon + \tfrac{1}{8}\epsilon^2 + O(\epsilon^4), \\ A_v &\sim -\tfrac{1}{4}\epsilon + \tfrac{1}{8}\epsilon^2 + O(\epsilon^4), \\ \bar{q} &\sim \tfrac{1}{2}[1 - \tfrac{3}{4}\epsilon^2 + \tfrac{3}{4}\epsilon^3 + O(\epsilon^4)], \end{aligned}\right\} \tag{45}$$

which places the virtual control at the foot of the sill on the dense reservoir side ($x_v = -1$). Similarly for the very high sill, $D_w \to \infty$, we can show

$$\left.\begin{aligned} A_c &\sim -0.12544, \\ A_v &\sim \tfrac{1}{2} - 0.35104/D_w, \\ \bar{q} &\sim 0.41598. \end{aligned}\right\} \tag{46}$$

Again $x_v = -1$. The height of the interface above the datum at the virtual (foot) control is independent of the depth of the channel at that section in the asymptotic limit.

For general D_w the value of A_c will lie between zero and $A_{c\infty} = A_c(D_w = \infty) = -0.12544$, while A_v will be bounded between zero and $\frac{1}{2} - 0.35104/D_w$. Figures 8 and 9 show plots of the exact solutions (evaluated numerically) for A_c, A_v and $\bar{q}$, along with the asymptotic solutions from (45) and (46). It is clear from both plots that most of the changes in the flow are associated with only a small increase in the depth of the channel away from the sill crest. If the channel deepens by around 25% away from the crest A_c is within approximately 17% of its $D_w \to \infty$ value; the exchange flow rate takes somewhat longer to approach its large D_w asymptotic value.

Note how well (45) matches the exact value for A_c even for D_w much greater than that for which it is formally valid. The deviation is less than 10% for D_w between 1 and 2.5, by which point the true value of A_c is within 3% of its large D_w asymptotic

value. Unfortunately both the interface height coefficient at the virtual (foot) control and the exchange flow rate are not such good fits. However, if the asymptotic value for A_c is used in (28), rather than an asymptotic approximation to this equation, a more accurate value for $\bar{q}$ may be obtained.

The hydraulic results are in agreement with Armi & Farmer (1986) who looked at channels of constant depth ($D_w = 1$) and Farmer & Armi (1986) who investigated sills whose depth went to infinity ($D_w \to \infty$) before widening. They did not consider intermediate channels with the sill rising from finite depth. We have shown here that the $D_w \to \infty$ limit is a good model if D_w is greater than around 1.5, and that the constant-depth model should be applied with caution as small departures from constant depth lead to a relatively large response by the flow.

6.2. *Net flow*

The response to net flow of controlled flow over a simple sill is more complicated than that through a channel of constant depth. Depending on the height of the sill and the strength of the forcing, the flow may behave like either the unforced flow over a simple sill or the forced flow through a channel of constant depth. The feature which distinguishes these two types of behaviour is the position of the virtual control. We shall use the term *contraction-like behaviour* to describe flows in which the virtual control is upstream (with respect to the net barotropic flow) of the sill crest, positioned somewhere in the expanding region of the channel. *Sill-like behaviour* has the virtual control located as a foot (exit) control at $x = -1$ on figure 7, as would be the case if there were no net flow. The solution to $K = 0$ at the virtual control is due to the $\partial J/\partial b$ term vanishing for contraction-like behaviour, and both $\mathrm{d}b/\mathrm{d}x$ and $\mathrm{d}D/\mathrm{d}x$ vanishing for sill-like behaviour. A third type of behaviour, *coincident behaviour*, is also possible; this will be explained in more detail later.

Numerical evaluation of the hydraulic solutions is necessary except when the forcing is sufficiently strong to bring one or the other of the layers to rest. Calculation of these values may be carried out by putting $Q = \pm\bar{q}$ and $A_v = \pm\frac{1}{2}$ into (26) and (28) and equating for the two control sections. For $Q > 0$ the upper layer is brought to rest at the same net forcing, $Q = Q_t = (2D_c/3)^{\frac{3}{2}} b_c$, independently of the value of D_w. The virtual control is positioned out in the dense reservoir where $b_v = \infty$. At the crest $A_c = \frac{1}{6}$. Thus regardless of the value of D_w the channel will exhibit contraction-like behaviour if the net flow is sufficiently strong.

When the forcing is from the light reservoir ($Q < 0$), the lower layer is first brought to rest when $Q = -(\frac{2}{3}D_w)^{\frac{3}{2}} b_c$, corresponding to $A_c = \frac{1}{2} - \frac{2}{3}D_w$ provided $D_w < \frac{3}{2}D_c$. Under these conditions the flow exhibits contraction-like behaviour with the front forming at the virtual control with $b_v = \infty$. In contrast, if $D_w \geqslant \frac{3}{2}D_c$, the lower layer will vanish at the sill crest before the front could form in the light reservoir. Thus we see coincident behaviour where the front forms at the sill crest with the primary and virtual controls coinciding at that point. The forcing required is $Q = -D_c^{\frac{3}{2}} b_c = -\bar{q}_{\max}$.

As the flow demonstrates sill-like behaviour when $Q = 0$, if either contraction-like or coincident behaviour is exhibited when one of the layers is brought to rest, at some value of the net forcing there must be at least one transition from one type of behaviour to another. The flow requires the exchange flow rate to be a continuous function of Q, and hence will remain continuous over such a transition. In contrast the position of the virtual control need not be a continuous function of Q, and so the configuration of the interface may show a sudden change if the virtual control were to jump from one side of the primary control to the other.

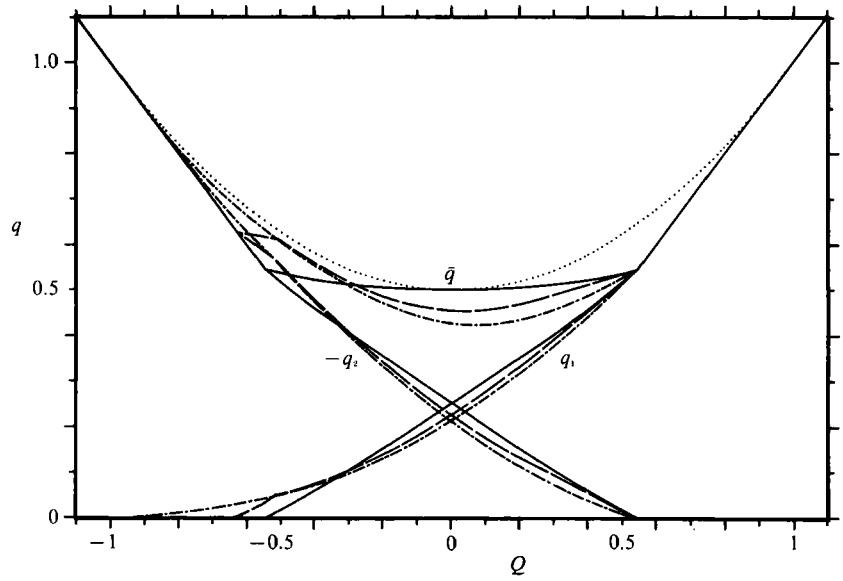

FIGURE 10. The effect of net barotropic forcing on the flow rates over a simple sill. Solid lines for $D_w = 1$; long dashes for $D_w = 1.1$; dot-dash for $D_w = 1.5$. The exchange flow rate, if the two controls were to coincide at the sill crest, is plotted also (dotted line).

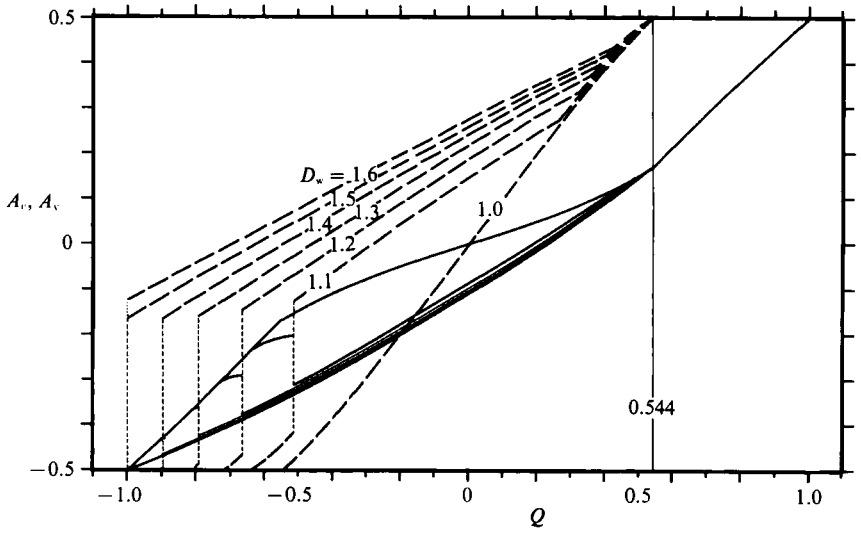

FIGURE 11. Variations in the interface height coefficient at the sill crest (A_c, solid lines) and virtual control (A_v, dashed lines) as a function of the net barotropic forcing. The value of D_w (sill geometry) is marked on the A_v curves. Transitions from contraction-like to sill-like behaviour (for $Q < 0$) are shown by vertical dashed lines. For $Q > 0$ the transitions correspond to sudden changes in $\partial A_v/\partial Q$.

Figure 10 shows how the exchange flow rate varies with the net barotropic forcing for a number of different values of D_w. Notice the transition from sill-like to contraction-like behaviour for $Q < 0$ with $D_w = 1.1$ (dashed lines) results in a sharp change in the slope of the flow rates. This is to be expected as $\bar{q}$ is the envelope of solutions with the virtual control at $x_v = -1$ (sill-like) and those with $x_v > 1$ (contraction-like). The discontinuity in $\partial\bar{q}/\partial Q$ does not occur for the transition from

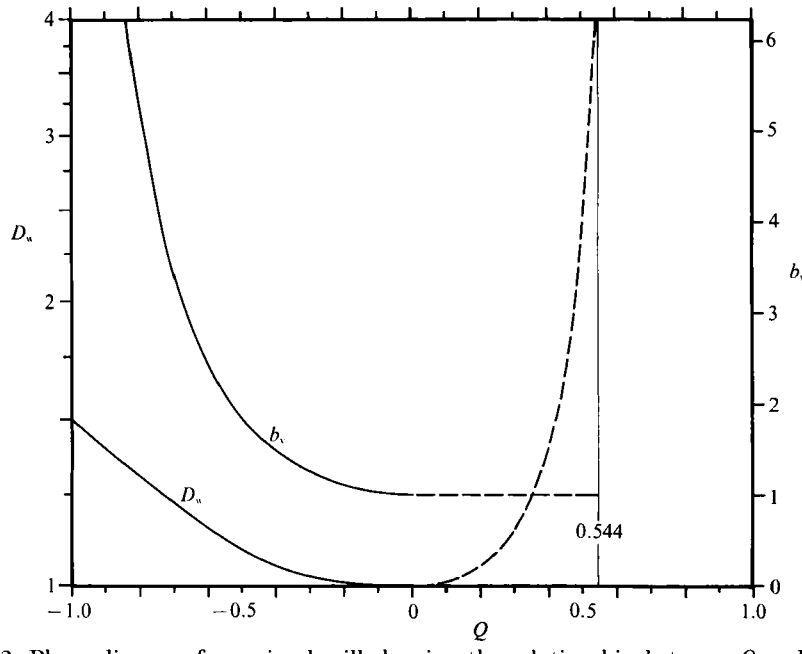

FIGURE 12. Phase diagram for a simple sill showing the relationship between Q and D_w for the transition from contraction-like (below D_w curve) to sill-like (above D_w curve) behaviour. The width at the virtual control for the contraction-like solution, at this transition, is also plotted (b_v curve). Solid lines for $Q < 0$ indicate that the transition causes a jump in the values of A_c and A_v; dashed lines for $Q > 0$ indicate that no such jump occurs.

sill-like to contraction-like behaviour for $Q > 0$. The virtual control remains at $x = -1$ until Q reaches some threshold value for which $\partial J/\partial b$ vanishes at $x = -1$. Increasing Q further allows x_v to move out from $x = -1$ towards the denser reservoir. For comparison $\bar{q}_{max}$, the value $\bar{q}$ would take if both controls were at the sill crest, is also shown in figure 10 (dotted line). For $D_w = 1.5$ (dot-dash line), $\bar{q} = \bar{q}_{max}$ when $Q = -1$ and the transition from sill-like to coincident behaviour occurs with both controls positioned at the crest of the sill.

The height coefficients at the primary (solid lines) and virtual (dashed lines) controls are shown in figure 11 as a function of the net barotropic forcing for a number of different values of D_w. Notice the discontinuities in both A_c and A_v at the transition from sill-like to contraction-like behaviour for $Q < 0$. Even though the exchange flow rate is a continuous function of the net forcing, the interface profile is not. Some care should be exercised in considering the discontinuity in A_v as a significant portion of this is due to the associated jump in x_v from $x_v = -1$ to $x_v > 1$. The primary control coefficient A_c is always evaluated in the same position and so gives a better indication of the overall jump in the interface configuration associated with a change in the net forcing. There is no jump in A_c for the transition from sill-like to coincident behaviour. The transition to contraction-like behaviour for $Q > 0$ is marked by a sharp change in $\partial A_v/\partial Q$, corresponding to x_v becoming a varying function of Q, though the changes in A_c remain smooth.

Figure 12 is a phase diagram for the flow over a simple sill showing the relationship between D_w and Q at which the transition from sill-like to contraction-like behaviour occurs. The corresponding width at the virtual control (for the contraction-like branch) is also plotted. The corresponding values of the interface height coefficients

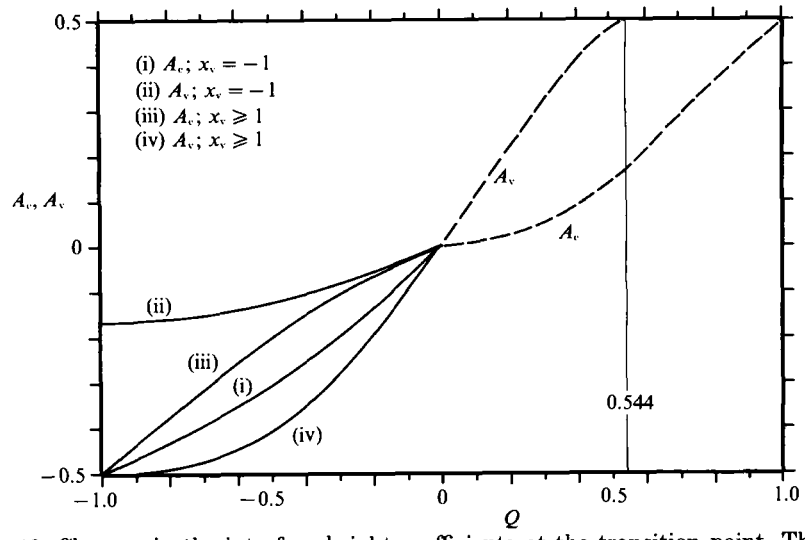

FIGURE 13. Changes in the interface height coefficients at the transition point. The channel is a simple sill with D_w such that for the given value of Q the flow is at the transition between the types of behaviour. Thus the difference between curves (i) and (iii) and between (ii) and (iv) represent the jump in the interface height due to the transition from sill-like to contraction-like behaviour. For $Q > 0$ (shown dashed) there is no jump.

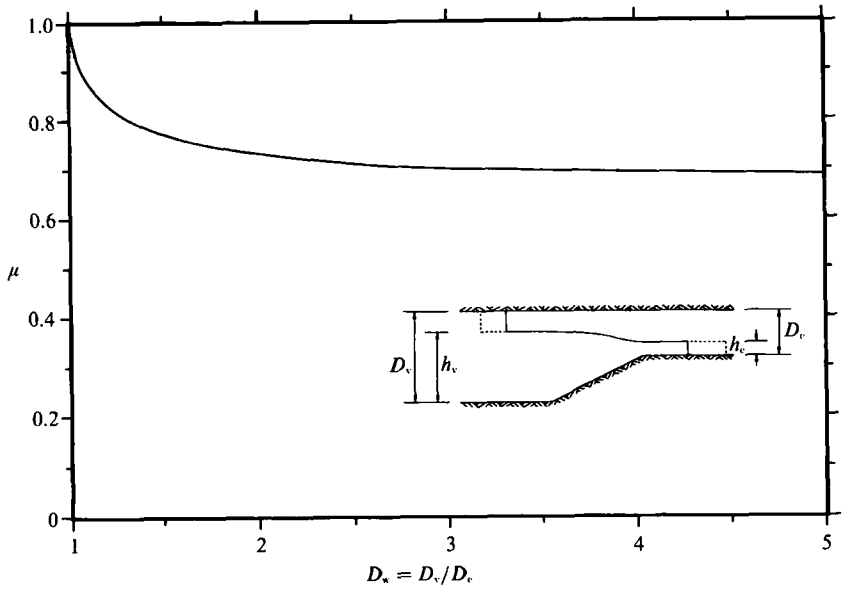

FIGURE 14. Dissipation coefficient (μ) for the flow over a sill as a function of the sill geometry (D_w). Set-up is from rest.

are shown in figure 13. For $Q < 0$ the values of A_c and A_v are given for both types of behaviour. The curves are shown dashed for $Q > 0$ where there is no jump associated with the transition.

In the limits $D_w = 1$ and $D_w = \infty$, the present analysis reproduces the results of Farmer & Armi (1986). The results for finite sill heights and transitions in the behaviour of the flow are new.

6.3. *Dissipation*

Some early workers in two-layer hydraulics used energy conservation arguments to determine the flow along a channel of uniform cross-section (e.g. Yih 1965, p. 136). They stated that the rate at which the kinetic energy of the mean motion increases ($\dot{E}_k$) is equal to the rate at which potential energy is released ($\dot{E}_p$) for a mutual intrusion along a channel. Subsequently other authors (e.g. Whitehead *et al.* 1974) have attempted to apply this to more general channel flows. It is therefore of interest to determine whether or not similar arguments may be applied to the set-up from rest of two-layer flows over sills.

In this analysis we shall consider only situations in which there is no net flow. The simplest channel geometry containing the essential features of the hydraulically controlled flow over a sill is one with $D(x) = D_w$ for $x < x_v$ and $D(x) = 1$ for $x > x_c$ ($x_v < x_c$). The depth of the channel decreases between x_v and x_c in a smooth, monotonic manner. Suppose that initially the fluid is at rest with a barrier dividing the dense and light fluids within the channel. At $t = 0$ the barrier is removed and the interface adjusts itself. Sometime after the flow has established, we may calculate the rate of increase in the kinetic energy and decrease in the potential energy from the conditions at x_c and x_v. In terms of the interface height coefficients at the primary and virtual (foot) controls, we define

$$\mu = \frac{\dot{E}_k}{\dot{E}_p},$$

$$= \frac{D_c^{-2}[(\frac{1}{2}+A_c)^{-2}+(\frac{1}{4}-A_c^2)^{-1}]+D_v^{-2}[(\frac{1}{2}-A_v)^{-2}+(\frac{1}{4}-A_v^2)^{-1}]}{D_c(\frac{3}{2}-A_c)-D_v(\frac{1}{2}-A_v)}\bar{q}^2. \tag{47}$$

When $\mu = 1$ there is no dissipation; $\mu < 1$ represents dissipation during the set-up process and continued dissipation at any propagating head of the flow or hydraulic jumps in reservoirs. As the flow over a sill is controlled at x_c and x_v, we may use the hydraulic solutions to determine μ. The resultant value of μ is plotted in figure 14 as a function of D_w. When $D_w = 1$ the coefficient μ is unity, indicating that the flow is energy conserving. For $D_w > 1$, μ is less than unity, demonstrating that dissipation or radiation of energy by waves must occur during the set-up process from dam break (and a wide variety of other initial conditions). In the limit as $D_w \to \infty$, $\mu \to 0.6623$.

Only in the case of a channel with symmetry about a horizontal plane is it possible to equate the rate of gain of kinetic energy with the rate of release of potential energy ($\mu = 1$). Similar arguments apply to the adjustment process from any arbitrary initial state, or to channels of constant depth when $Q \neq 0$.

7. Partial control

This section looks briefly at what happens when hydraulic control is lost at one of the control sections. Gill (1977) reviewed single-layer hydraulic theory and showed that over a wide range of conditions the surface height in the downstream reservoir could only be matched onto by the formation of a hydraulic jump in the supercritical region of the flow. Only if the surface height was equal to that associated with subcritical flow into the reservoir would there be a smooth transition from upstream to downstream reservoirs. In such a situation the flow would be subcritical everywhere.

For two-layer hydraulics the situation is essentially similar, although the addition of a second supercritical solution branch makes the picture a little more complex.

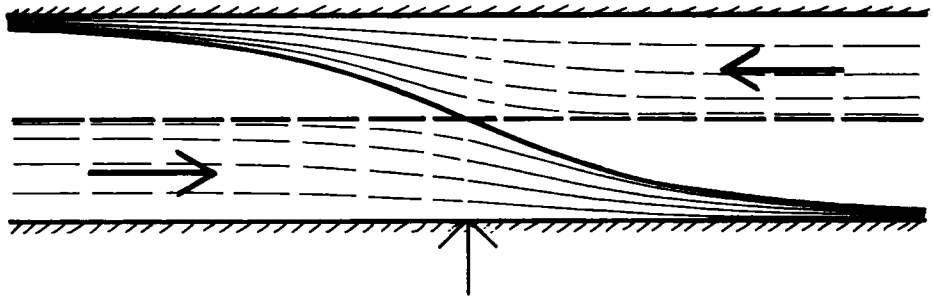

FIGURE 15. Interface profiles for flow through a channel of constant depth. The heavy lines denote the fully controlled (maximal) solution and its associated subcritical root. Light lines represent submaximal flows. Continuous lines indicate supercritical solution branches and dashed lines subcritical branches. See text for more details.

The statement by Armi & Farmer (1986) that the interface height in the reservoirs cannot be on the wrong side (i.e. lower for the dense reservoir or higher for the light reservoir) of the interface height at the virtual control is correct although may be a little confusing. For this present discussion we shall assume that the dense reservoir (the reservoir in which the interface height $H+h$ is greater) is to the left. While our discussion will be confined to channels of constant depth and simple sills without any net flow, more complex geometries and net flow may be treated in a manner similar to the flow over a simple sill.

Solution for a flow that is subcritical everywhere is trivial in the geometries we are considering. The inherent symmetry (with respect to x) of the channel and the unique subcritical solution to $J = 0$ requires the interface height in the two reservoirs to be identical. There is no potential energy to drive a flow and so the fluid will be motionless everywhere. Purely subcritical uncontrolled solutions therefore have little relevance to real flows. Any difference in interface height will introduce one or more hydraulic transitions.

Figure 15 shows a range of possible interface profiles, in a channel of constant depth, for a range of different reservoir conditions. Solid lines represent supercritical solution branches and dashed lines subcritical branches. Heavy lines represent the unique fully controlled (maximal) solution and its associated subcritical root. All interface profiles have a hydraulic transition at the contraction.

If the interface height in the left-hand (dense) reservoir is above the half-depth point of the channel, then it may only be matched onto from the supercritical branch of the flow by a hydraulic jump. There are no subcritical flows – other than those that are subcritical everywhere – able to match onto such reservoir conditions. Similarly, if the interface height in the right-hand (light) reservoir is below the half-depth point of the channel, then a hydraulic jump is required to match onto it from the supercritical flow into it. If the hydraulic jump is induced by friction rather than the level of the interface in the reservoir, the fluid may undergo a number of further hydraulic transitions and jumps before entering the reservoir.

An interface height in the dense reservoir above the half-depth point and in the light reservoir below the half-depth point can only be matched onto by a fully controlled flow with two (coincident) hydraulic transitions at the contraction (heavy continuous line in figure 15). In contrast, if the level of the interface in the dense reservoir lies below the half-height point (i.e. the subcritical solution branch associated with the fully controlled flow; heavy dashed line in figure 15), a subcritical solution exists which is able to match the flow onto the conditions in the dense

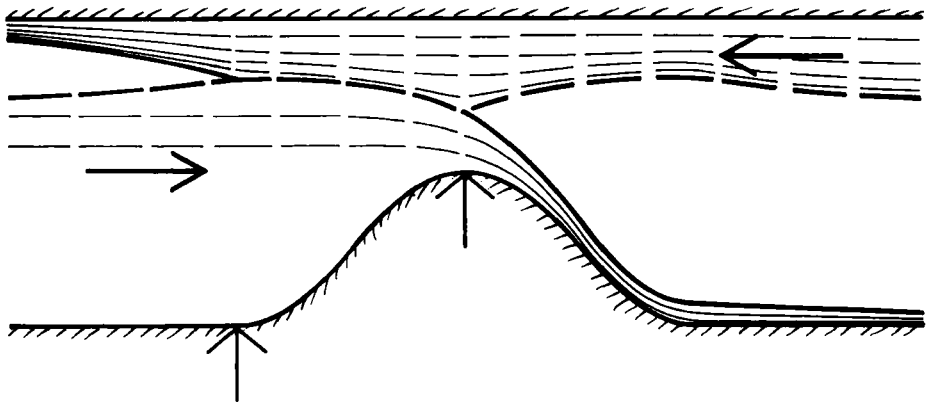

FIGURE 16. Interface profiles for flow over a simple sill. The heavy lines denote the fully controlled (maximal) solution and its associated subcritical root. Light lines represent sub maximal flows. Continuous lines indicate supercritical solution branches and dashed lines subcritical branches. See text for more details.

reservoir. This solution has a single hydraulic transition at the contraction and may match onto the conditions within the light reservoir through a hydraulic jump (light lines in figure 15). Similarly, if the interface height in the light reservoir is above the half-height point the flow is subcritical to the right of the contraction and supercritical to the left. A jump may then form to match onto the dense reservoir.

In figure 4 we plotted how the exchange flow rate for critical conditions varied as a function of A at any section (the discussion in §4.3 was for a sill but the shape of the curve applies equally to any along-channel geometry). Since the flow is critical at the contraction for all the solutions plotted in figure 15, the curve of figure 4 shows how the exchange flow rate changes between the fully controlled and partially controlled solutions. The fully controlled solution has $A_c = 0$ which maximizes $\bar{q}_{crit}$. All the partially controlled solutions have $|A_c| > 0$ and so the exchange flow is submaximal.

The situation is more complicated when there is a net barotropic flow or variations in the channel depth. To illustrate this we shall consider no net flow over a sill. Figure 16 plots interface profiles for a sill with a range of different reservoir conditions. As with the channel of constant depth, the crucial factor is the relationship between the height of the interface in the reservoirs and the position of the subcritical solution branch associated with the fully controlled flow (heavy dashed line). If the interface in the dense reservoir lies above this line, then the only way of matching a flow onto it is through a hydraulic jump. Similarly, if the interface in the light reservoir is below this line, then again a hydraulic jump is required. When both these conditions hold the flow is fully controlled with control sections at the sill crest and the foot of the sill on the side of the dense reservoir.

If the interface in the dense reservoir were to fall below the associated subcritical branch of the fully controlled flow, the hydraulic control at the foot control would be flooded. The flow would then be subcritical everywhere to the left of the sill crest. The single hydraulic transition over the crest produces a supercritical flow towards the light reservoir which may subsequently be matched onto the reservoir conditions through a hydraulic jump. The value of A_c is displaced further from A_{max} at the sill crest by these partially controlled flows, reflecting their submaximal character.

If the interface in the light reservoir is above the heavy dashed line in figure 16 then the control at the sill crest is flooded. The flow everywhere to the right of the

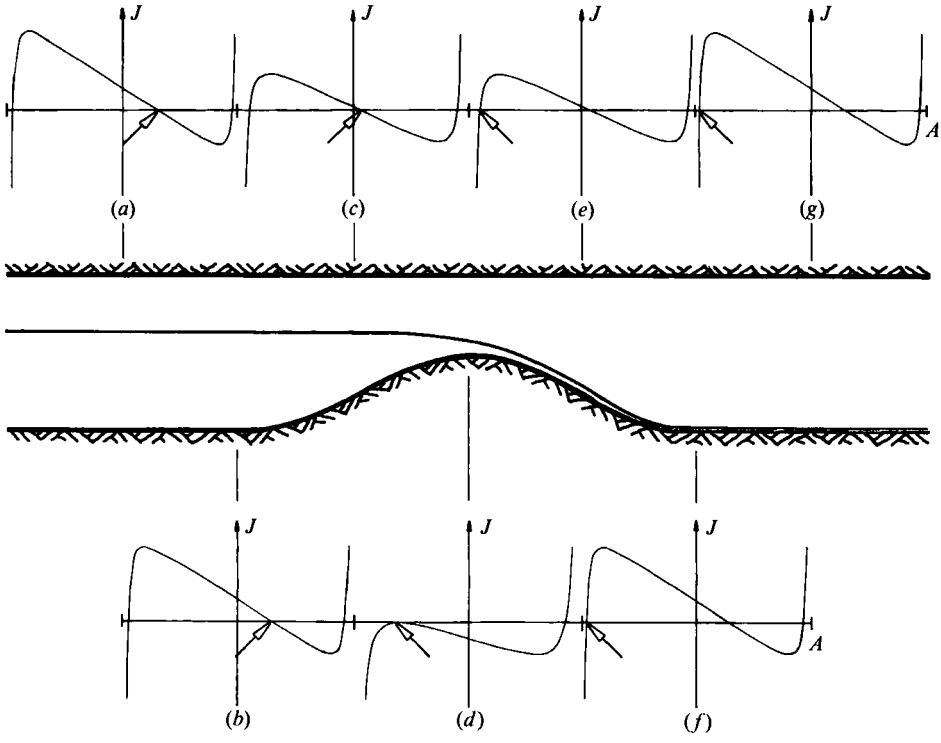

FIGURE 17. Variations in the hydraulic functional for a partially controlled flow over a simple sill. The geometry of the channel is identical to that in figures 2 and 3. The functional is plotted for the positions indicated above and below the channel. The A-axis of these plots goes from $-\frac{1}{2}$ to $\frac{1}{2}$. The appropriate root of $J = 0$ is indicated by an arrow. Critical conditions occur only at the sill crest (section d). The flow is subcritical ($\partial J/\partial A < 0$) everywhere to the left of the crest.

remaining control at the foot of the sill (on the dense reservoir side) is subcritical (the flow is, in fact, critical at the foot on the light reservoir side, but a hydraulic transition is unable to occur at this point). The transition then allows a supercritical flow into the dense reservoir to form which may be matched onto the reservoir through a hydraulic jump. The value of A_v at the virtual (foot) control is displaced further from A_{max} at this point, again showing the partially controlled solution to be submaximal (conditions are not critical at the sill crest so a value of A closer to A_{max} at this point is of no consequence).

The solution process for submaximal flows is to solve $J = 0$ simultaneously for the reservoir and a single control at which $\partial J/\partial A = 0$. The position of this single control will be such that $\bar{q}$ is minimal for all possible positions. Any other position would not allow the solution to be traced back towards the subcritical reservoir. Figure 17 demonstrates how $J(\cdot\,; A)$ varies along the channel for a partially controlled flow with the flow subcritical between the dense reservoir and the sill crest. This figure is the submaximal equivalent of figure 2.

8. Conclusions

In this paper we have demonstrated the application of Gill's (1977) functional formalism to two-layer exchange flows. The approach illuminates the requirements for the flow to be realizable more clearly than the Froude-number-plane formulation

used by previous authors. The functional framework provides a more flexible tool for handling hydraulic problems, particularly when the along-channel geometry is of a complex form (Dalziel 1988).

Maximal exchange is confirmed for fully controlled flows. If only one hydraulic transition is present (partially controlled flow) then the exchange flow rate is submaximal. Submaximal flow will occur if the conditions in one of the reservoirs cannot be matched onto by a hydraulic jump from the fully controlled flow.

The fully controlled flow has been shown to be very sensitive to small departures from symmetry about a horizontal plane in the along-channel geometry. For the simple sill geometry adopted in this paper, the asymmetry introduced by the sill causes the two controls to separate, one remaining at the sill crest and the other moving to the foot of the sill on the dense-reservoir side (when $Q = 0$). As the depth at the foot of the sill increases relative to that at the crest, the solution very rapidly approaches that for infinite depth at the foot of the sill. If the difference is around 50% of the depth at the crest, then the position of the interface and the strength of the exchange flow rate are within 10% of their values for an infinitely high sill. The displacement of the interface from the mid-depth point at the crest is around 13% of the channel depth and the exchange flow rate is reduced by around 17%, when there is no net flow, compared with a channel without variations in the depth. Farmer & Armi's (1986) use of the $D_w \to \infty$ limit is therefore valid for many real flows. However, the $D_w = D_c$ limit should be applied with caution as only small departures from constant depth produce quite large differences in the flow.

In the case of cold air intruding into a warm room, the position of the interface between warm and cold air will be displaced upward from mid-door height if the height of the doorway is less than the ceiling height within the room. If the doorway is less than around 75% the height of the ceiling, the interface will be displaced upwards by around $\frac{1}{8}$ of the height of the doorway (in the absence of a net flow). While this rough analysis assumes that there are two homogeneous layers and negligible vertical velocities (neither of which is strictly true for real flow through a doorway), it never the less gives a qualitative description of the observed behaviour (Steckler, Baum & Quintiere 1984; Dalziel 1988; Dalziel & Lane-Serff 1990).

When a net barotropic flow is added to the flow over a simple sill some novel features have been found. If the net flow is sufficiently weak, the flow behaves much like that with $Q = 0$, although the interface is displaced upward ($Q > 0$) or downward ($Q < 0$). The controls are positioned at the sill crest and the foot on the dense reservoir side of the sill. However if the net flow is sufficiently strong, the channel may start to behave more like a contraction with $Q \neq 0$: the effect of the depth variations are swamped by the variations in the width of the bounding channel with the virtual control moving into the expanding region away from the sill. Whether this behaviour occurs depends on the strength and direction of the net forcing and the depth away from the crest of the sill. For $Q < 0$ there is a jump in the position of the interface associated with the transition from sill-like to contraction-like behaviour, though this will only occur if the depth away from the crest is less than $1\frac{1}{2}$ times the depth at the crest. If the depth away from the crest is greater than this and $Q = -(\frac{2}{3}D_c)^{\frac{3}{2}} g'^{\frac{1}{2}} b_c$, the lower layer is brought to rest with both controls at the crest of the sill; there is no jump in the interface profile associated with the transition to this behaviour from sill-like behaviour at smaller $|Q|$. The transition in behaviour for $Q > 0$ will always occur if Q is sufficiently strong, though in this case there is no corresponding jump in the interface profile.

Finally, the strengths of the hydraulic functional are not confined to rectangular

cross-sections or non-rotating channels. The derivation, features and solution process outlined in §4 may be applied equally to channels of non-rectangular cross-sections and rotating channels. The relationship between the composite Froude number and J proves to be a particularly useful tool for rotating channels where defining an appropriate Froude number is not straightforward. Non-rectangular cross-sections and rotating channels are covered by Dalziel (1988, 1990).

This work was undertaken while I was in receipt of a Commonwealth Scholarship as a postgraduate student at the University of Cambridge. I am grateful to the Association of Commonwealth Universities for this opportunity, and to my supervisor over this time, Dr Paul Linden, for his continued help and guidance.

REFERENCES

ARMI, L. 1986 The hydraulics of two flowing layers of different densities. *J. Fluid Mech.* **163**, 27–58.

ARMI, L. & FARMER, D. M. 1986 Maximal two-layer exchange through a contraction with barotropic net flow. *J. Fluid Mech.* **164**, 27–51.

ARMI, L. & FARMER, D. M. 1987 A generalisation of the concept of maximal exchange in a strait. *J. Geophys. Res.* **92** (C 13), 14679–14680.

ARMI, L. & FARMER, D. M. 1988 The flow of Atlantic water through the Strait of Gibraltar. *Prog. Oceanogr.* **21**, 1–105.

DALZIEL, S. B. 1988 Two-layer hydraulics: maximal exchange flows. PhD thesis, Department of Applied Mathematics and Theoretical Physics, University of Cambridge.

DALZIEL, S. B. 1990 Rotating two-layer sill flows. In *The Physical Oceanography of Sea Straits* (ed. L. J. Pratt). NATO/ASI Series. Kluwer.

DALZIEL, S. B. & LANE-SERFF, G. F. 1990 The hydraulics of doorway exchange flows. *Building and Environ.* (to appear).

FARMER, D. M. & ARMI, L. 1986 Maximal two-layer exchange over a sill and through the combination of a sill and contraction with barotropic flow. *J. Fluid Mech.* **164**, 53–76.

GILL, A. E. 1977 The hydraulics of rotating-channel flow. *J. Fluid Mech.* **80**, 641–671.

LAWRENCE, G. A. 1985 The hydraulics and mixing of two-layer flow over an obstacle. PhD thesis, Hydraulic Engineering Laboratory, University of California, Berkeley.

LONG, R. R. 1956 Long waves in a two-fluid system. *J. Met.* **13**, 70–74.

MEHROTRA, S. C. 1973 Boundary contractions as controls in two layer flows *J. Hydraul. Div. ASCE* **99** (HY11), 2003–2012.

PRATT, L. J. 1984 On nonlinear flow with multiple obstructions. *J. Atmos. Sci.* **41**, 1214–1225.

PRATT, L. J. & ARMI, L. 1987 Hydraulic control of flows with nonuniform potential vorticity. *J. Phys Oceanog* **17**, 2016–2029.

STECKLER, K. D., BAUM, H. R. & QUINTIERE, J. G. 1984 Fire induced flows through room openings – flow coefficients. *Rep.* NBSIR 83-2801, National Bureau of Standards, US Department of Commerce.

STOMMEL, H. & FARMER, H. G. 1953 Control of salinity in an estuary by a transition. *J. Mar. Res.* **12**, 13–20.

WHITEHEAD, J., LEETMAA, A. & KNOX, R. 1974 Rotating hydraulics of strait and sill flows. *Geophys. Fluid Dyn.* **6**, 101–125.

WOOD, I. R. 1968 Selective withdrawal from a stably stratified fluid. *J. Fluid Mech.* **32**, 209–223.

WOOD, I. R. 1970 A lock exchange flow. *J. Fluid Mech.* **42**, 671–687.

YIH, C. 1965 *Dynamics of Nonhomogeneous Fluids.* Macmillan.